CHAPTER IV
RESULTS AND DISCUSSION

This chapter presents the results obtained from the in vitro evaluation of the capsaicin-loaded transdermal nanofiber patch and discusses the significance of the findings in the context of its potential for pain relief applications. The study involved the formulation of nanofiber patches incorporating capsaicin, and subsequent biological assessments including cytotoxicity (MTT assay) and anti-inflammatory activity (*COX-2* inhibition) in human dermal fibroblast (HDF) cells.

Table 4.1 Experimental design and testing workflow for evaluation of capsaicin-loaded nanofiber patch

Parameter	Purpose/Design	Result/Outcome
Polyvinyl Alcohol (PVA)	Polymer matrix for nanofiber fabrication	Formed smooth nanofibers when mixed with PVP
Polyvinylpyrrolidone (PVP)	Co-polymer for nanofiber formulation	Enhanced fiber formation and drug dispersion
Capsaicin (CAP)	Active compound	Successfully encapsulated, bioactive in patch
Materials	PVA+PVP	Formed nanofibers when mixed
Materials	PVA+PVP+Capsaicin (Active compound)	20 g of PVA, 20 g of PVP+ 0.1 mg/ml of Capsaicin
Nanofibers	Diameter 500-1000 nm	667 ± 19.5 nm
Physicochemical Characterizations	FTIR SEM	- Identify and confirm the functional groups and - Distribution of nanofibers
Cytotoxicity assay	MTT assay (Nontoxic)	Nontoxic (< 10 mg/ml)

Table 4.1 Experimental design and testing workflow for evaluation of capsaicin-loaded nanofiber patch (Continued)

Parameter	Purpose/Design	Result/Outcome
Anti-Inflammatory Activity Test in Human Dermal Fibroblast (HDF) Cells	Cyclooxygenase-2 (*COX-2*) Inhibitory Activity	*COX-2* inhibition, anti-inflammatory effect
***In vitro* skin permeation**	Franz cell diffusion	The permeation of capsaicin through the Strat-M™ membrane
	FTIR, HPLC	FTIR spectral analysis revealed time-dependent variations in signal intensity, indicating progressive diffusion of capsaicin into deeper membrane layers.

4.1 Results

4.1.1 The Fabrication of CAP/PVA/PVP Nanofibers

In this study, capsaicin (CAP)-loaded nanofibers were successfully fabricated using a blend of polyvinyl alcohol (PVA) and polyvinylpyrrolidone (PVP) via electrospinning. The preparation of the polymer solution was performed by dissolving 20 g of PVA powder in a binary solvent system comprising 45 mL of distilled water and 45 mL of absolute ethanol, yielding a final concentration of 20% w/v. The solution was stirred at 80 °C for 3 hours using an electromagnetic stirrer until a clear, homogenous solution was obtained. Likewise, 20 g of PVP was dissolved under the same solvent conditions and stirred at 60 °C for 3 hours, resulting in a similarly transparent and uniform solution. The two polymer solutions were then mixed in equal volumes to achieve a final concentration of 10% w/v for both PVA and PVP, forming a stable polymeric matrix suitable for electrospinning.

Capsaicin was incorporated into the mixed polymer solution at a concentration of 0.1 mg/mL, corresponding to 10% v/w relative to the total polymer content. The final CAP/PVA/PVP solution was allowed to cool to room temperature

and rested for several hours to ensure complete homogenization before proceeding to electrospinning, as previously described by Hindi et al. (2021).

The electrospinning process was conducted at room temperature using a 10 mL disposable syringe fitted with a metal needle with an internal diameter of 0.55 mm. The polymer solution was loaded into the syringe and extruded at a flow rate of 3 mm/hr using a syringe pump. An electric voltage of 15 kV was applied across a 17-cm tip-to-collector distance. The nanofibers were collected on aluminum foil affixed to a rotating cylindrical drum collector, which ensured consistent fiber deposition and alignment.

The electrospun fibers appeared continuous, uniform, and free from visible bead formation, indicating that the process parameters solvent system, polymer concentration, applied voltage, flow rate, and distance were well optimized. The combination of PVA and PVP offered a favorable balance of viscosity, conductivity, and mechanical properties, enabling stable electrospinning and nanofiber formation, highlighting the compatibility of PVA/PVP blends in producing nanofibers with smooth morphology.

The successful fabrication of CAP-loaded nanofibers under these optimized conditions establishes a foundational step for further physicochemical and biological characterization. Subsequent studies were focus on evaluating fiber morphology using scanning electron microscopy (SEM), drug release kinetics, and biological efficacy to validate the application of this formulation as a transdermal system for pain relief.

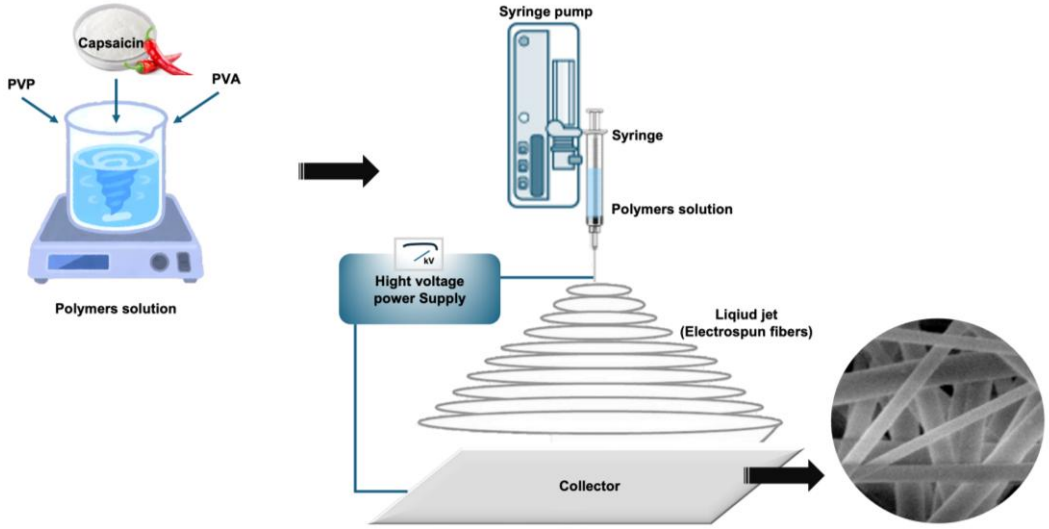

Figure 4.1 Schematic representation of the electrospinning process used to fabricate CAP/PVA/PVP nanofibers

The process involves applying a high-voltage electric field to a polymer solution loaded in a syringe, resulting in the formation of continuous nanofibers collected on a grounded rotating drum. The accompanying histograms illustrate the distribution of fiber diameters, confirming uniform morphology and consistent nanofiber formation.

4.1.2 Physicochemical Characterizations

Figure 4.2 displays the Fourier-transform infrared (FT-IR) spectra of of polyvinyl alcohol (A), polyvinylpyrrolidone (B), capsaicin (C), and the capsaicin-loaded nanofibers patch (D). These spectra were used to identify and confirm the functional groups of capsaicin and to determine whether capsaicin remained chemically stable after incorporation into the nanofiber matrix.

In the spectrum of pure capsaicin (Figure 4.2C), the broad absorption peak observed at approximately 3300 cm^{-1} corresponds to O–H stretching, indicative of phenolic hydroxyl groups. The bands at 2923 cm^{-1} and 2854 cm^{-1}represent asymmetric and symmetric C–H stretching vibrations of aliphatic $–CH_2$ and $–CH_3$ groups. A sharp peak at around 1640 cm^{-1} corresponds to C=O stretching of the amide group, while the peaks in the region of 1510–1450 cm^{-1} are attributed to aromatic C=C ring

stretching vibrations. Additional peaks near 1260 cm^{-1} and 1020 cm^{-1}can be assigned to C–N stretching and C–O stretching, respectively, confirming the characteristic structure of capsaicin.

The FT-IR spectrum of the capsaicin-loaded nanofibers patch (Figure 4.2D) shows several overlapping and shifted peaks, consistent with the successful incorporation of capsaicin into the polymer matrix. The broad O–H stretching band at 3300 cm^{-1} is retained, though broadened, indicating hydrogen bonding interactions between capsaicin and the polymeric components particularly PVA and PVP. The peaks at 2925 cm^{-1} and 2850 cm^{-1}, corresponding to aliphatic C–H stretching, were also observed, confirming the presence of capsaicin within the patch.

Notably, the carbonyl stretching band (1640 cm^{-1}) was slightly shifted and broadened in the nanofiber spectrum, suggesting possible physical interactions between the capsaicin and the hydroxyl or carbonyl groups present in the polymers. This interaction implies molecular entrapment rather than covalent bonding, which is desirable for controlled drug release without altering drug activity.

In the fingerprint region (1200–700 cm^{-1}), characteristic peaks associated with the PVP and PVA backbone such as C–O, C–C, and C–N stretching were clearly evident, confirming the structural integrity of the polymer network post-electrospinning. Importantly, no new peaks or significant changes were detected, indicating that capsaicin remained chemically stable and did not undergo degradation during the fabrication process.

These findings confirm the successful physical incorporation of capsaicin into the nanofiber matrix, while preserving its functional groups and overall chemical structure. The observed shifts in peak position and intensity further support the existence of non-covalent interactions, such as hydrogen bonding, between capsaicin and the polymer system. Such interactions are advantageous for sustained drug release and stability within the patch formulation.

Overall, FT-IR analysis validated the chemical compatibility of capsaicin with the PVA/PVP polymer blend and demonstrated that the electrospinning process did not alter the integrity of the bioactive compound.

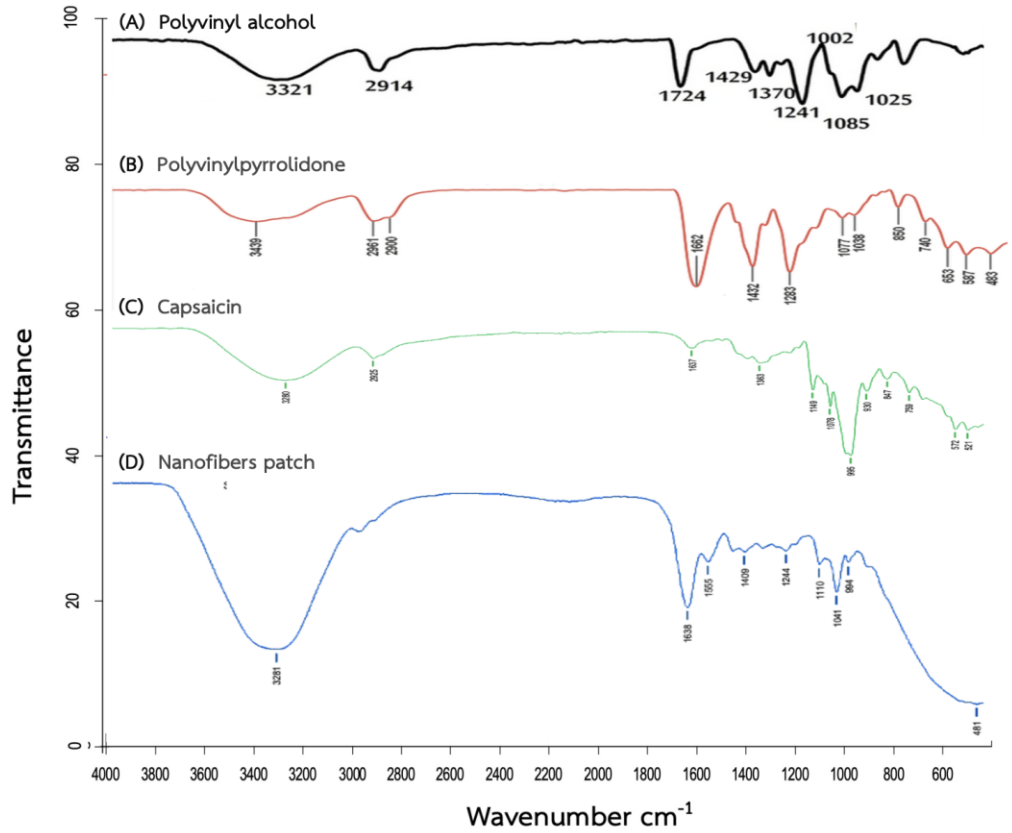

Figure 4.2 FT-IR spectrum and chemical formula of polyvinyl alcohol (A), polyvinylpyrrolidone (B), capsaicin (C), and nanofibers patch (D)

4.1.3 Surface Morphology Characterizations (SEM)

The surface morphology of nanofibers was evaluated by using the scanning electron microscope (SEM). The average diameter distribution of nanofibers was calculated by image analysis software. The nanofiber specimen was sputter coated with platinum before subjecting to the SEM imagery (Hindi et al., 2021).

The morphology of the capsaicin-loaded nanofibers was investigated using Scanning Electron Microscopy (SEM), as shown in Figure 4.4A. The image captured at 5,000× magnification revealed that the nanofibers were smooth, continuous, and bead-free, indicating a homogenous polymer solution and well-optimized electrospinning parameters as shown in Figure 4.3. The fibers appeared randomly oriented but uniformly distributed, which is desirable for consistent drug release and mechanical performance in transdermal applications. The fiber diameters were quantitatively analyzed using ImageJ software (NIH, USA), based on SEM images. A total

of 50 randomly selected fibers were measured, and the results are illustrated in the histogram in Figure 4.3B. The fiber diameters followed a unimodal, slightly right-skewed distribution. The mean fiber diameter was found to be 0.667 ± 0.195 μm, which is equivalent to 667 ± 19.5 nanometers (nm). This confirms that the fibers fall well within the nanoscale range (1–1000 nm), validating the successful formation of true nanofibers.

The relatively narrow standard deviation indicates high uniformity of fiber thickness, which is essential for ensuring consistent surface area for drug release, mechanical stability, and patch flexibility. The absence of bead formation also suggests favorable polymer–solvent interactions and appropriate electrospinning voltage and flow rate settings. In comparison with other capsaicin-loaded nanofiber systems reported in the literature, the fiber diameter obtained in this study is comparable or smaller, suggesting enhanced surface-area-to-volume ratio, which may contribute to improved drug dispersion and skin permeation performance. These morphological characteristics confirm the suitability of the CAP/PVA/PVP nanofiber formulation for transdermal delivery applications. The incorporation of capsaicin into the polymeric matrix appears homogeneously distributed throughout the fibers, indicating successful encapsulation and suggesting a potential for sustained drug release across the membrane.

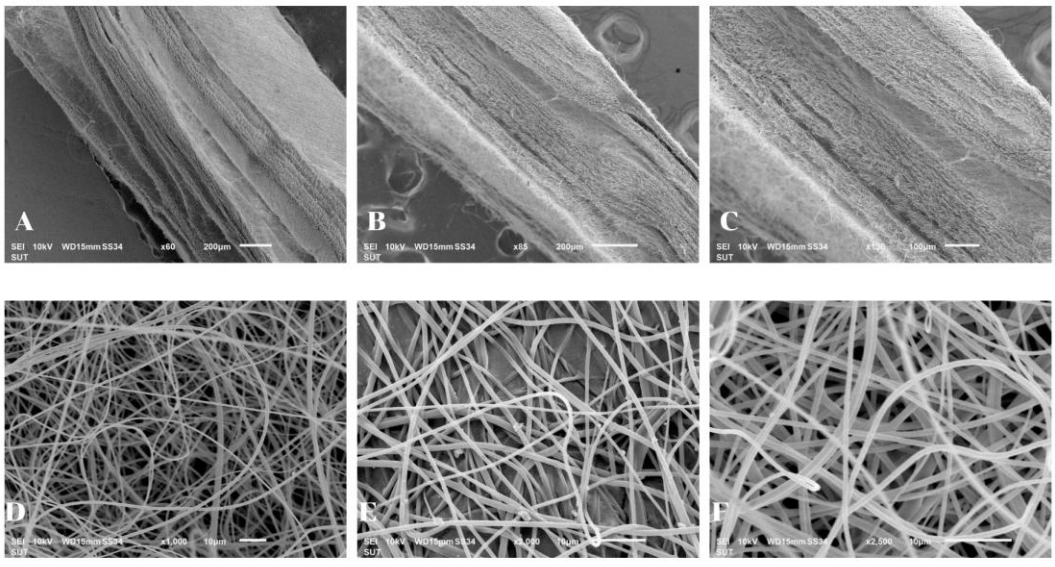

Figure 4.3 SEM micrographs of capsaicin-loaded nanofiber patch and skin interface

(A–C) Cross-sectional SEM images of skin after transdermal patch application at different magnifications (A: ×60, B: ×85, C: ×130). These images demonstrate the interaction of the fibrous layer can be seen adhering to the outer skin layer. (D–F) SEM images of the surface morphology of electrospun nanofibers at increasing magnifications (D: ×1,000, E: ×2,000, F: ×2,500). The capsaicin nanofibers incorporated show a continuous, bead-free, and smooth structure with randomly oriented networks, which is favorable for high surface area and effective drug loading and release.

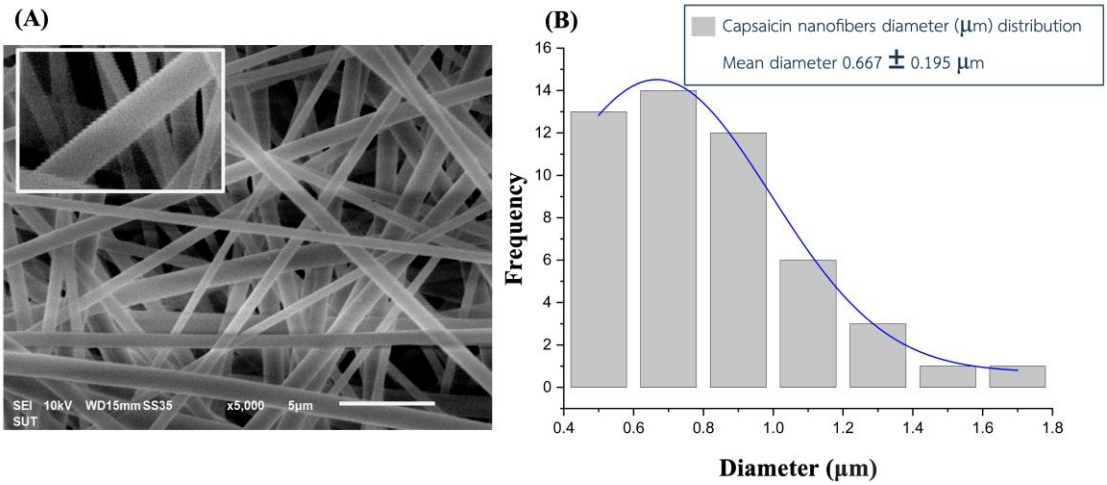

Figure 4.4 Surface morphology of nanofibers

(A) Scanning Electron Microscopy (SEM) image of capsaicin-loaded nanofibers at 5,000× magnification, showing uniform and bead-free morphology. (B) Diameter distribution histogram of capsaicin nanofibers, with a mean diameter of 0.667 ± 0.195 µm, indicating consistent fiber formation with a slight right-skewed distribution.

4.1.4 Cytotoxicity assay

Cytotoxicity Evaluation of Capsaicin-Loaded Nanofiber Patch on Human Dermal Fibroblasts (HDF)

The cytotoxicity of the capsaicin-loaded nanofiber patch was evaluated on human dermal fibroblast (HDF) cells using the MTT assay, and the results are shown in Figure 4.5. Cells were treated with varying concentrations of nanofiber extract (0.0001 to 100 mg/mL) for 24 hours.

At lower concentrations (0.0001–1 mg/mL), the nanofiber extract did not exhibit cytotoxic effects. In fact, at 0.001 and 0.01 mg/mL, a significant increase in cell viability was observed ($p < 0.001$), with viability exceeding 130% relative to the untreated control group. This suggests that low concentrations may not only be safe but also potentially promote fibroblast activity or exert mild protective effects, possibly due to the antioxidant and anti-inflammatory properties of capsaicin at sub-cytotoxic levels.

Conversely, at higher concentrations (10–100 mg/mL), a dose-dependent decrease in cell viability was observed. Cell viability dropped to approximately 75% at 50 mg/mL and further declined to ~40% at 100 mg/mL ($p < 0.001$), indicating notable cytotoxic effects at elevated doses. From the dose–response curve, the half-maximal inhibitory concentration (IC_{50}) was estimated to be approximately 20 mg/mL, which defines the concentration at which capsaicin causes a 50% reduction in cell viability under these *in vitro* conditions.

This IC_{50} value provides a useful benchmark for establishing the upper safety limit for formulation development. Notably, the concentrations that showed any cytotoxicity (≥10 mg/mL) are significantly higher than those typically used in in vivo transdermal delivery, where localized drug concentrations on the skin surface are much lower due to controlled release and limited permeation. Clinical formulations of capsaicin patches (e.g., 0.025–0.1% w/w) correspond to microgram-per-milliliter levels once applied to skin, which are well below the IC_{50} threshold observed here.

Therefore, the capsaicin nanofiber patch demonstrates a wide safety margin for dermal application, and concentrations effective in pain relief are expected to remain well within the non-cytotoxic range *in vivo*. These findings confirm the biocompatibility of the formulation and support its potential for further development as a safe transdermal therapeutic system.

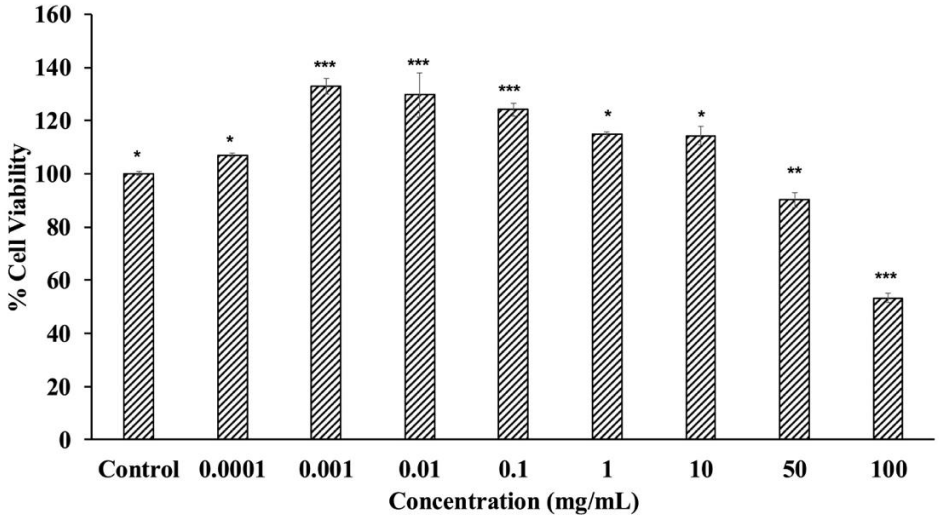

Figure 4.5 Human dermal fibroblasts (HDF) cells treatment with nanofiber patch Using the MTT Assay

The bar graph illustrates the percentage of cell viability in HDFs treated with different concentrations of capsaicin (ranging from 0.0001 to 100 mg/mL), as measured by the MTT assay. Results are expressed as a percentage relative to the untreated control group (100%).

At low concentrations (0.001–0.1 mg/mL), capsaicin significantly enhanced cell viability compared to the control, suggesting a stimulatory or protective effect on HDFs (*$p < 0.05$, **$p < 0.01$, ***$p < 0.001$). However, at higher concentrations (50–100 mg/mL), a significant decrease in cell viability was observed, indicating dose-dependent cytotoxicity. Notably, the viability dropped below 80% at 50 mg/mL and further to around 60% at 100 mg/mL, showing potential toxicity at these levels. These findings support the use of low-dose capsaicin for therapeutic applications with minimal cytotoxic risk.

4.1.5 Investigation of Cyclooxygenase-2 (*COX-2*) Inhibitory Activity for Analgesic Properties

To assess the anti-inflammatory efficacy of the capsaicin-loaded nanofiber patch, gene expression analysis of cyclooxygenase-2 (*COX-2*) was performed using quantitative real-time polymerase chain reaction (qRT-PCR) in human dermal fibroblast (HDF) cells. The *GAPDH* gene was used as an internal reference for normalization.

As shown in Figure 4.6, exposure of HDF cells to hydrogen peroxide (H_2O_2, 1 mM) resulted in a marked increase in *COX-2* expression, approximately 3.5-fold higher than in the untreated control group. This significant upregulation confirmed that H_2O_2 effectively induced oxidative stress and mimicked an inflammatory microenvironment within the fibroblast population. *COX-2* is a key inducible enzyme involved in the biosynthesis of pro-inflammatory prostaglandins and is commonly used as a molecular marker for inflammatory activity.

In contrast, treatment with the capsaicin-loaded nanofiber patch at a concentration of 0.1 mg/mL following H_2O_2 stimulation led to a significant downregulation of *COX-2* mRNA expression. Quantitative analysis showed that *COX-2* levels were reduced by approximately 8.1-fold when compared to the H_2O_2-treated group. This robust suppression indicates that the patch formulation effectively mitigates inflammation at the transcriptional level. The observed reduction in *COX-2* expression is consistent with the known mechanisms of capsaicin, which include inhibition of pro-inflammatory signaling pathways such as NF-**K**B and MAPKs. Capsaicin is also known to modulate oxidative stress and reduce the expression of downstream inflammatory mediators, making it a promising candidate for topical anti-inflammatory therapy.

The successful delivery of capsaicin via the nanofiber matrix likely contributed to its enhanced bioavailability and sustained action at the cellular level. The polymer blend of PVA/PVP may also have supported the biological compatibility of the patch, allowing for efficient interaction with the cell membrane and intracellular uptake. These findings demonstrate that the capsaicin-loaded nanofiber patch possesses significant anti-inflammatory potential by downregulating *COX-2* expression in inflamed dermal cells. The patch could thus serve as an effective non-NSAID alternative for managing localized inflammation, such as in myofascial pain syndrome (MPS) or other soft tissue inflammatory conditions. Further validation through in vivo experiments is warranted to confirm therapeutic efficacy and pharmacodynamic behavior.

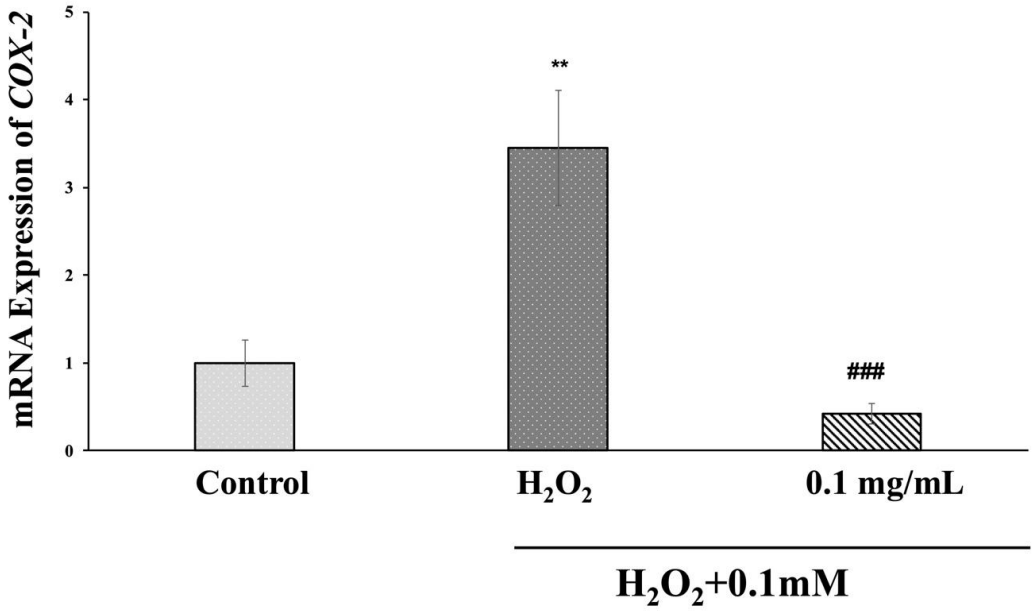

Figure 4.6 Evaluation of Anti-inflammatory Activity in HDF Cells by Real-Time PCR Targeting Two Genes (*GAPDH* and *COX-2*)

The bar graph illustrates the relative mRNA expression levels of cyclooxygenase-2 (*COX-2*) in human dermal fibroblasts (HDFs) under different treatment conditions. Exposure to 0.1 mM hydrogen peroxide (H_2O_2) significantly upregulated *COX-2* expression compared to the untreated control (**$p < 0.01$). Treatment with the capsaicin nanofiber patch (0.1 mg/mL) in combination with H_2O_2 markedly reduced *COX-2* mRNA expression (###$p < 0.001$) compared to the H_2O_2-treated group alone, indicating a strong anti-inflammatory effect. Data are presented as mean ± SD.

Effects of Capsaicin-Loaded Nanofiber Patch on Cell Morphology in HDF Cells

The protective and restorative effects of the capsaicin-loaded nanofiber patch on human dermal fibroblast (HDF) morphology were evaluated under oxidative stress conditions using phase-contrast microscopy, as illustrated in Figure 4.6. In the control group, HDF cells exhibited a typical spindle-shaped fibroblastic morphology with clear cell borders, well-defined cytoplasm, and healthy adherence to the culture surface indicating normal cell integrity. Following exposure to 1 mM

hydrogen peroxide (H_2O_2), the cells displayed significant morphological alterations, including cell shrinkage, elongation, cytoplasmic condensation, and partial detachment. These changes are consistent with oxidative stress-induced cellular damage and inflammation. However, cells treated with the capsaicin-loaded nanofiber patch at 0.1 mg/mL after H_2O_2 induction showed a noticeable recovery of normal fibroblastic morphology in Figure 4.7. The cells appeared more elongated and better attached, with fewer signs of structural damage, suggesting that the patch formulation helped mitigate the harmful effects of oxidative stress and promoted cellular protection or recovery.

These visual observations align with gene expression results from the *COX-2* qRT-PCR analysis and further support the anti-inflammatory and cytoprotective role of capsaicin delivered via the nanofiber patch system.

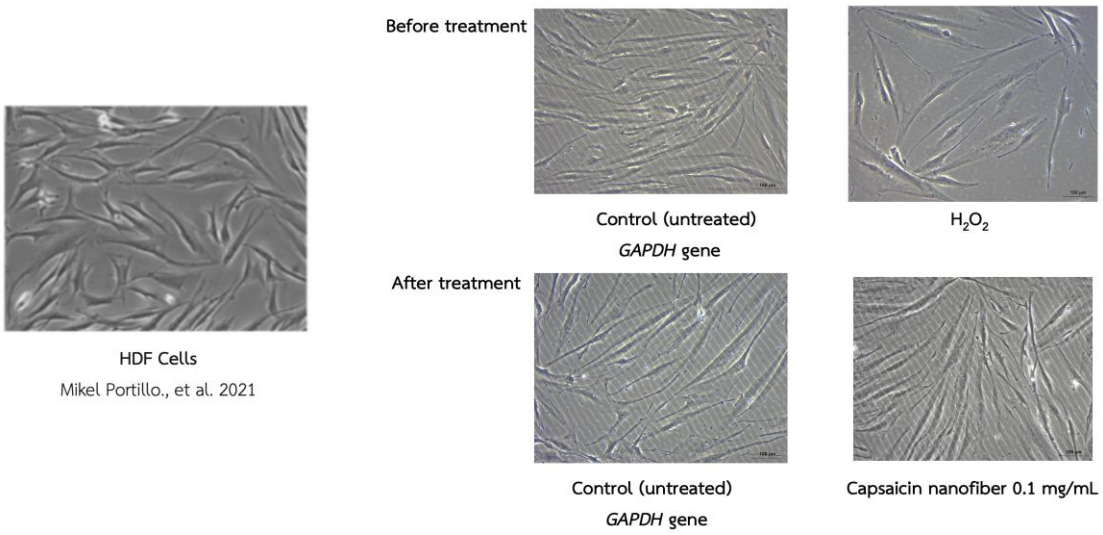

Figure 4.7 Morphological Observation of HDF Cells After Treatment with H_2O_2 and Capsaicin-Loaded Nanofiber Patch

This panel shows phase-contrast microscopy images illustrating the morphology of human dermal fibroblasts (HDFs) before and after treatment under different conditions.

When comparing the observed HDF morphology in this experimental image with the reference image from the following conclusions can be drawn:

Normal (Untreated) HDF Morphology: Both control groups (before and after treatment) and the reference image exhibit classic spindle-shaped, elongated fibroblast morphology with well-organized alignment. This confirms that the cultured HDFs maintain normal cell characteristics under non-stressed conditions, consistent with Portillo et al.'s report.

H_2O_2-Treated Cells: this study shows clear morphological deterioration cells appear rounded, detached, and fragmented, contrasting sharply with the healthy reference cells. This supports that oxidative stress induces significant cellular damage, disrupting the fibroblastic phenotype.

Capsaicin Nanofiber Treatment (0.1 mg/mL): Cells partially regain their spindle-like shape and alignment after treatment, resembling the healthy morphology seen in Portillo et al., 2021. This suggests a restorative or protective role of capsaicin nanofibers against oxidative insult.

Conclusion: Compared to the morphological standard from (Portillo et al., 2021), these findings demonstrate that capsaicin nanofibers help maintain or restore HDF morphology under oxidative stress, providing visual evidence of cytoprotective efficacy.

4.1.6 High-performance liquid chromatography (HPLC) analysis

After a 12-hour skin permeation experiment, the surface of the skin was washed with deionized water and allowed to dry. Capsaicin content in the stratum corneum (SC) was determined via the tape-stripping method using 20 pieces of 3M Scotch Magic™ tape (1 × 1 cm). To assess capsaicin retention in the underlying skin layers, the remaining tape-stripped skin was minced. Extraction of capsaicin from the tape samples and minced tissue was carried out using a 1:1 (v/v) mixture of phosphate-buffered saline (PBS, pH 7.4) and absolute ethanol, with volumes of 5 mL and 2 mL, respectively. All samples were sonicated for 30 minutes, filtered, and analyzed by high-performance liquid chromatography (HPLC).

HPLC analysis was performed using an HP1100 system with UV detection at 280 nm. Separation was conducted on a Hypersil ODS column (250 × 4.0 mm i.d., 5 µm) with a mobile phase comprising acetonitrile and 1% acetic acid (1:1,

v/v) at a flow rate of 1.0 mL/min. The injection volume was set at 10 µL. Method validation confirmed the accuracy, precision, and linearity of capsaicin quantification. Calibration curves showed strong linearity as shown in Figure 4.8, and all measurements were performed in triplicate. The graph shows the linear relationship between capsaicin concentration (µg/mL) and peak area. The regression equation is y=0.05256x, y=0.05256x, with a correlation coefficient of R^2=0.99700, indicating excellent linearity across the tested range (50–500 µg/mL)

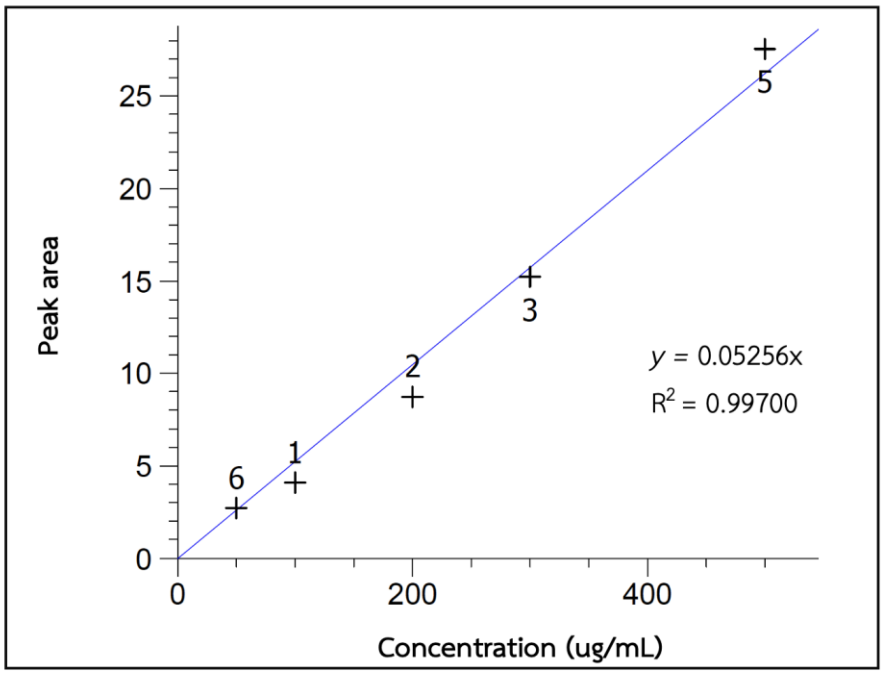

Figure 4.8 The standard calibration curve of capsaicin analyzed by HPLC

High-performance liquid chromatography (HPLC) was used to monitor capsaicin permeation through the skin at various time intervals: 1, 2, 4, 6, 8, and 12 hours. The chromatograms demonstrated consistent retention times for capsaicin, approximately between 22.3 and 22.6 minutes, across all time points, confirming the presence and stability of capsaicin in the samples. As shown in Figures 4.9–4.14, capsaicin was clearly detectable at each time point, with peak intensity correlating with permeation duration. The retention time and peak shape remained sharp and reproducible, indicating the robustness of the analytical method. The gradual increase

in peak area from 1 to 12 hours suggests a sustained release and continuous permeation of capsaicin through the skin model over time. This observation supports the potential of the tested transdermal delivery system for providing prolonged therapeutic effect. These findings are consistent with the chromatographic profile of standard capsaicin under identical HPLC conditions and confirm that capsaicin remains chemically stable throughout the 12-hour experimental period.

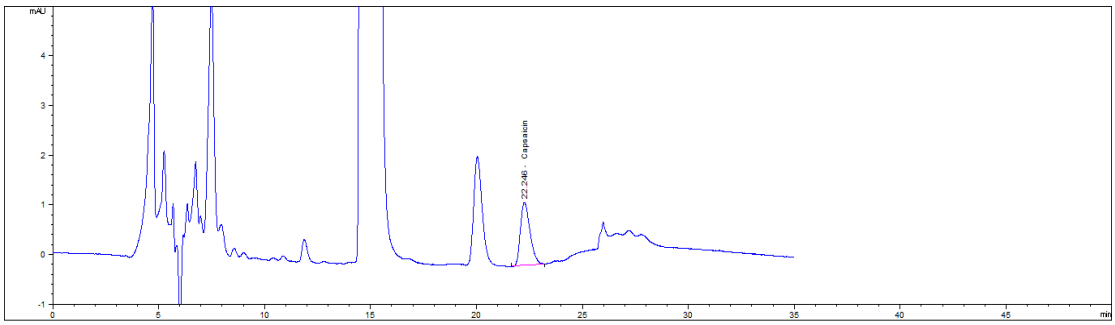

Figure 4.9 HPLC Chromatogram at 1 Hours Showing Capsaicin Retention Time

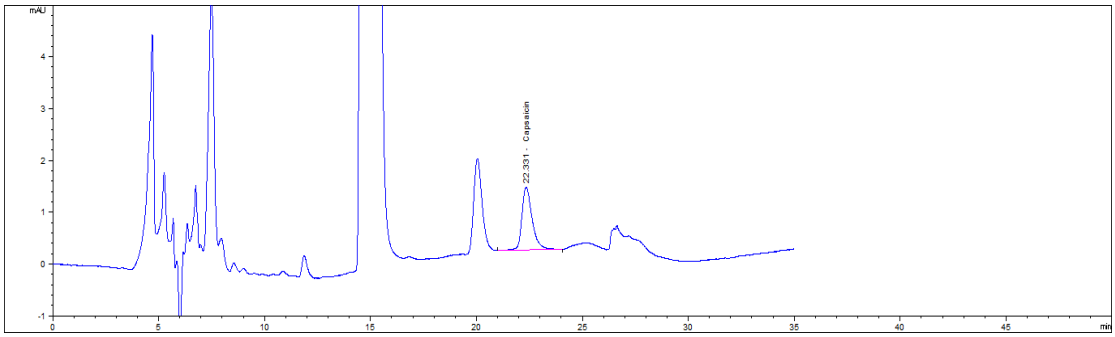

Figure 4.10 HPLC Chromatogram at 2 Hours Showing Capsaicin Retention Time

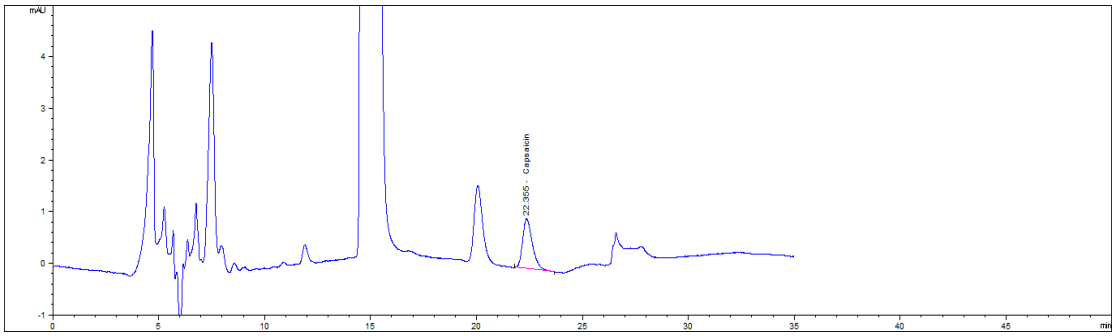

Figure 4.11 HPLC Chromatogram at 4 Hours Showing Capsaicin Retention Time

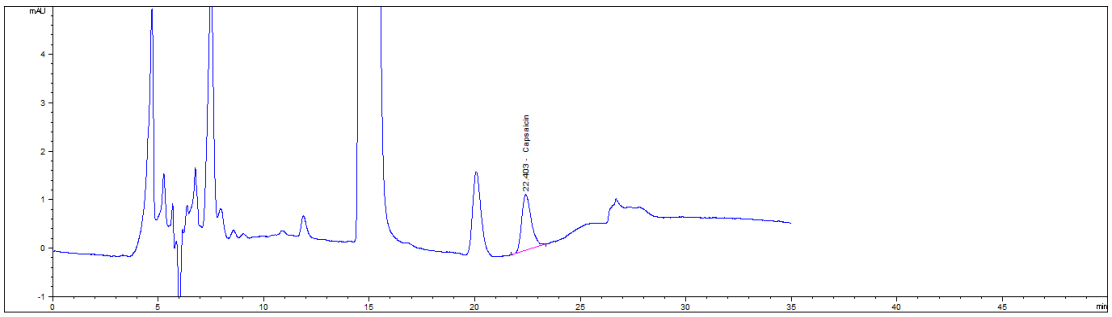

Figure 4.12 HPLC Chromatogram at 6 Hours Showing Capsaicin Retention Time

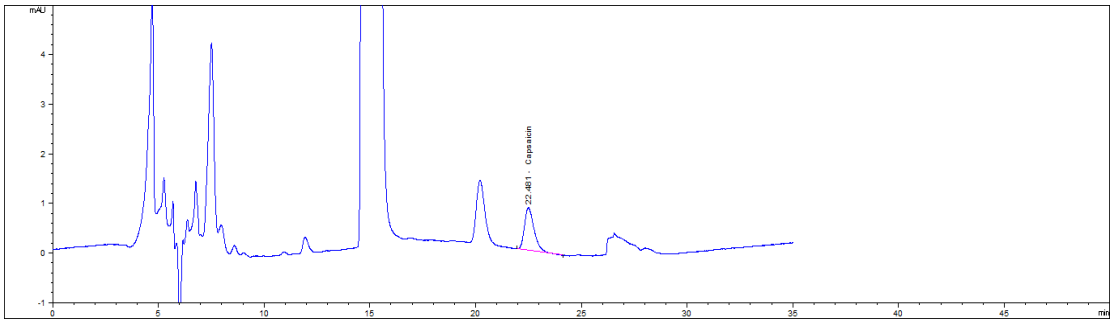

Figure 4.13 HPLC Chromatogram at 8 Hours Showing Capsaicin Retention Time

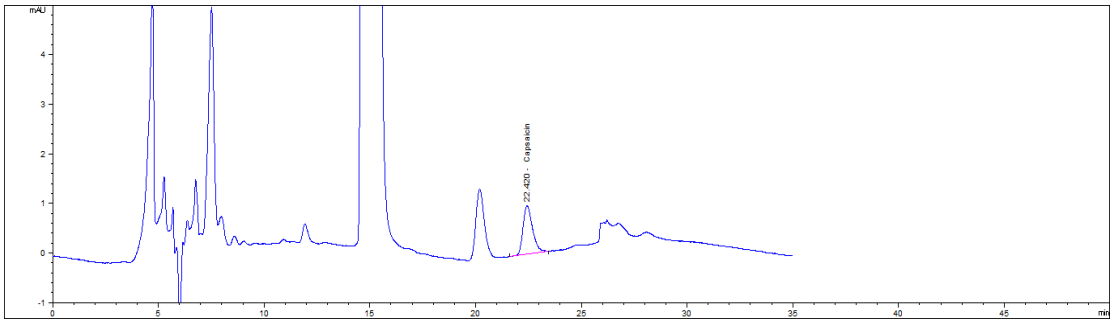

Figure 4.14 HPLC Chromatogram at 12 Hours Showing Capsaicin Retention Time

The permeation rate of capsaicin through the Strat-M™ membrane was determined by calculating the slope of the graph plotting the cumulative amount of capsaicin permeated against time (hours). The lag time corresponds to the x-intercept of the linear segment of this curve. The steady-state flux of capsaicin was then calculated using Equation (2), where steady-state flux (J_{ss}) is defined as the rate of change in cumulative permeation (dQ/dt) divided by the surface area (A) of the Strat-M™ membrane.

Steady state flux (Jss) = (dQ/dt)/A

= 63.30 µg/cm²/hr

The graph illustrates the relationship between the cumulative amount of capsaicin permeated per unit area (µg/cm²) and time (hours). The results demonstrate a consistent increase in permeation over a 12-hour period, indicating sustained drug release behavior. Notably, the time interval between 2 and 8 hours exhibits a clearly linear trend, suggesting that capsaicin permeation reached a steady-state phase during this period. Based on the slope of this linear portion, the steady-state flux (Jss) was calculated to be 63.30 µg/cm²/hr, reflecting the formulation's efficiency in delivering capsaicin across the Strat-M™ membrane via transdermal diffusion.

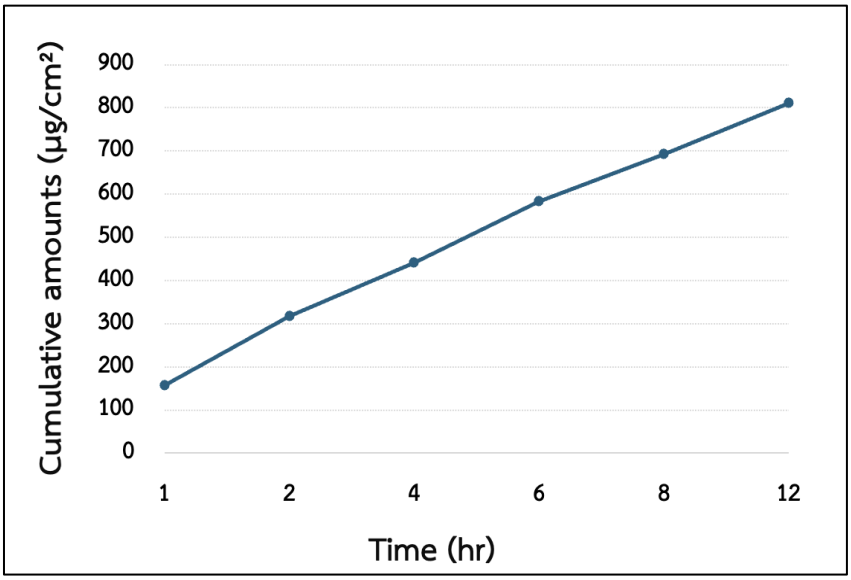

Figure 4.15 Cumulative Permeation of Capsaicin Through Strat-M™ Membrane

The graph illustrates the cumulative amount of capsaicin permeated per unit area (µg/cm²) over time, showing a sustained release profile. The linear segment between 2 and 8 hours was used to calculate the steady-state flux (J_{ss}).

The graph illustrates the permeability coefficient (K_p) of capsaicin through the Strat-M™ membrane over a 12-hour period as shown in Figure 4.16. The K_p value, which reflects the drug's ability to diffuse through the membrane relative to its donor concentration, demonstrates a clear time-dependent decline. At the 1-hour

mark, the K_p value was at its peak (~0.77 cm/hr), indicating a rapid initial permeation rate likely driven by a high concentration gradient and the availability of capsaicin on the membrane surface. During the first 2 to 4 hours, the K_p sharply decreased, suggesting a reduction in the diffusion driving force as the drug began to penetrate deeper into the membrane. Beyond 6 hours, the K_p values approached a plateau (~0.05–0.07 cm/hr), signifying the transition into a quasi-steady state of drug release. This behavior is consistent with Fick's First Law of Diffusion, where the rate of diffusion is proportional to the concentration gradient, which gradually diminishes over time as equilibrium is approached.

This trend reflects the controlled release characteristics of the capsaicin-loaded nanofiber patch, which initially releases the drug rapidly and then sustains a slower, more consistent permeation rate. Such a release profile is desirable in transdermal drug delivery systems designed for prolonged therapeutic effects, especially for conditions such as pain or inflammation.

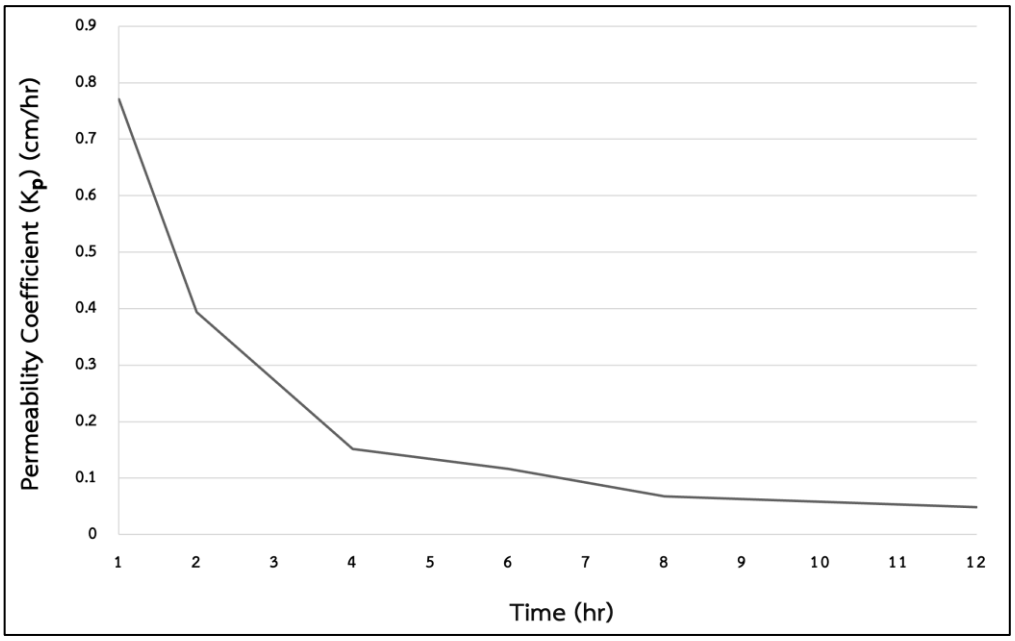

Figure 4.16 Permeability coefficient (K_p) of capsaicin from nanofiber patch over 12-hour transdermal diffusion

The graph shows the permeability coefficient (K_p) of capsaicin calculated at different time intervals (1–12 hr) based on transdermal permeation through the Strat-M™ membrane. The results illustrate an initial high K_p at 1 hour, followed by a gradual decline over time, indicating a transition from rapid to controlled drug release.

4.1.7 The *in vitro* skin permeation

The transdermal permeation of capsaicin from the nanofiber patch was evaluated using the Franz diffusion cell system, employing a Strat-M™ membrane as the skin model. Capsaicin concentrations within the stratum corneum were quantified using a tape-stripping method, while retention in the deeper dermal layers was assessed through a separate retention analysis.

FTIR microspectroscopy analysis: FTIR Imaging and Spectral Mapping of Strat-M™ Membrane Treated with Capsaicin Patch Compared to Control (1–12 hr). The FTIR imaging and spectral mapping of Strat-M™ membrane across different diffusion time points were used to monitor the permeation behavior and spatial localization of capsaicin through the membrane. The vibrational signals were analyzed and compared to the control to evaluate chemical penetration and retention over time. The cumulative amount of capsaicin permeated across the Strat-M membrane over a 12-hour period was determined and is illustrated in Figures 4.17-4.23 and APPENDIX B.

At 1 hr, strong FTIR absorption bands were observed near 2920–2850 cm^{-1} (C–H stretching) and 1650–1500 cm^{-1} (amide and aromatic groups), indicating early-stage surface adsorption of capsaicin. The chemical map shows high intensity in the upper region (epidermis-like layer), with little to no signal in deeper layers, suggesting minimal permeation.

After 2 hr, the spectral intensity in the upper layer slightly decreased, while signals extended deeper into the membrane. Increased peak intensity at 1250–1000 cm^{-1} (C–O and C–N stretching) reflected gradual permeation. The heatmap revealed more diffuse distribution compared to 1 hr.

At 4 hr, the chemical mapping indicates enhanced diffusion across the middle layer. The spectrum showed stronger intensity at 2920 cm^{-1} and 1030 cm^{-1},

which correspond to alkyl chains and ether groups from capsaicin, supporting deeper penetration.

At 6 hr, significant spectral intensity in the dermis-like layer was observed. Strong absorption at 1510 cm^{-1} (aromatic C=C) and 1100 cm^{-1}suggests active diffusion. The chemical map displays widespread distribution of capsaicin, indicating sustained release and permeation.

The FTIR at 8 hr profile reveals plateauing of permeation, with stable intensity across major peaks. Chemical imaging confirms accumulation in lower membrane layers, though peak shifts slightly suggest possible molecular interaction or binding with matrix components.

At 12 hr, capsaicin signal reached the deepest regions. The FTIR spectrum showed elevated intensity and broadened peaks, particularly around 1000–1100 cm^{-1}, indicating full-depth penetration. Compared to control (final image), the capsaicin-treated membrane demonstrates markedly higher chemical intensity and deeper spatial diffusion.

FTIR imaging and spectral analysis revealed the progressive permeation of capsaicin through the Strat-M™ membrane over a 12-hour period. At 1 hr, capsaicin signals were confined to the membrane surface (epidermis), with high intensity in C–H and amide regions. By 2–4 hrs, diffusion increased into the middle layers, with stronger C–O and C–N signals. At 6 hrs, capsaicin reached deeper (dermis-like) layers with enhanced aromatic and ether group peaks. At 8–12 hrs, full-depth permeation was observed, with broader and intensified peaks around 1000–1100 cm^{-1}, indicating maximal diffusion. Compared to the control, capsaicin-treated membranes showed significantly stronger and deeper chemical penetration.

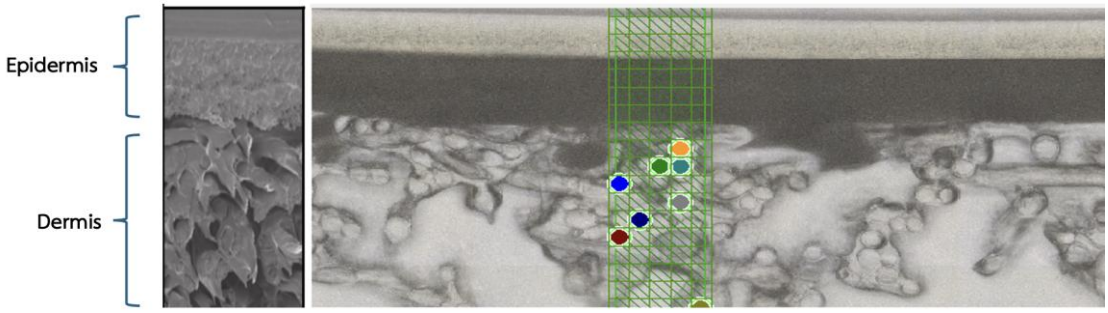

Figure 4.17 FTIR Imaging and Spectral Mapping of Strat-M™ Membrane

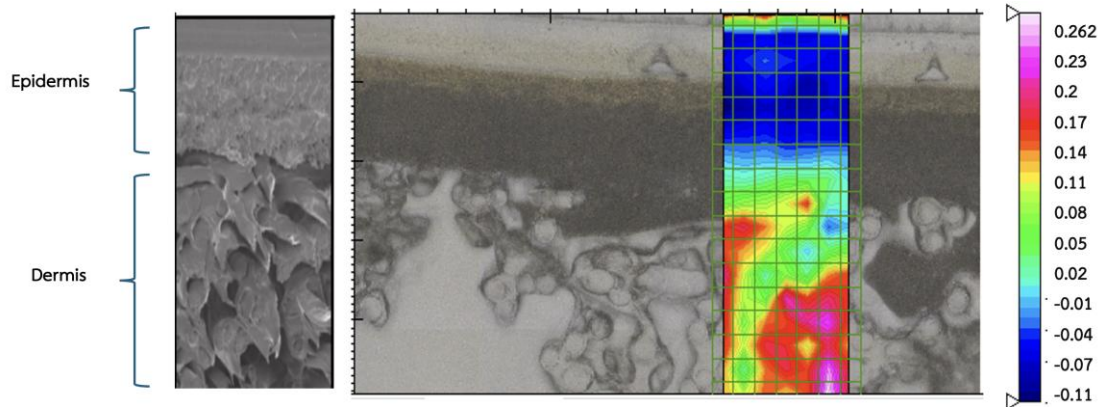

Figure 4.18 FTIR Imaging and Spectral Mapping of Strat-M™ Membrane at Various Time Points (1 hr) in Franz Diffusion Cell System

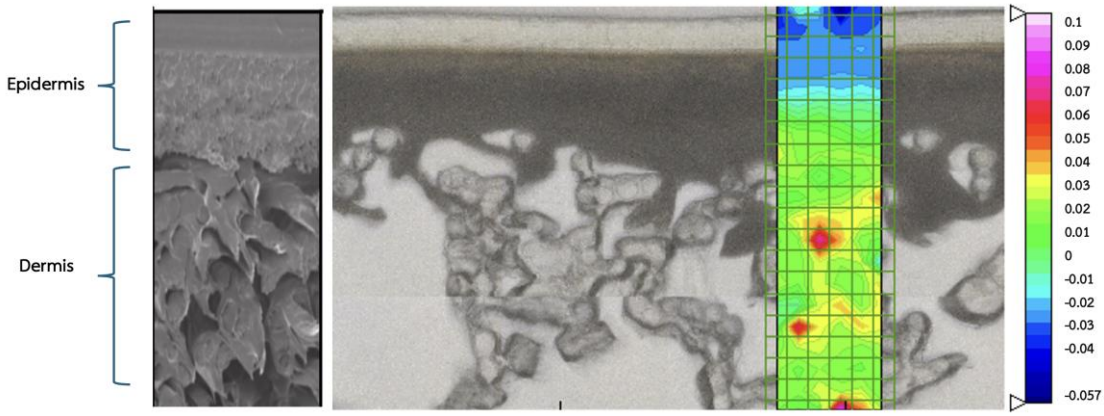

Figure 4.19 FTIR Imaging and Spectral Mapping of Strat-M™ Membrane at Various Time Points (2 hr) in Franz Diffusion Cell System

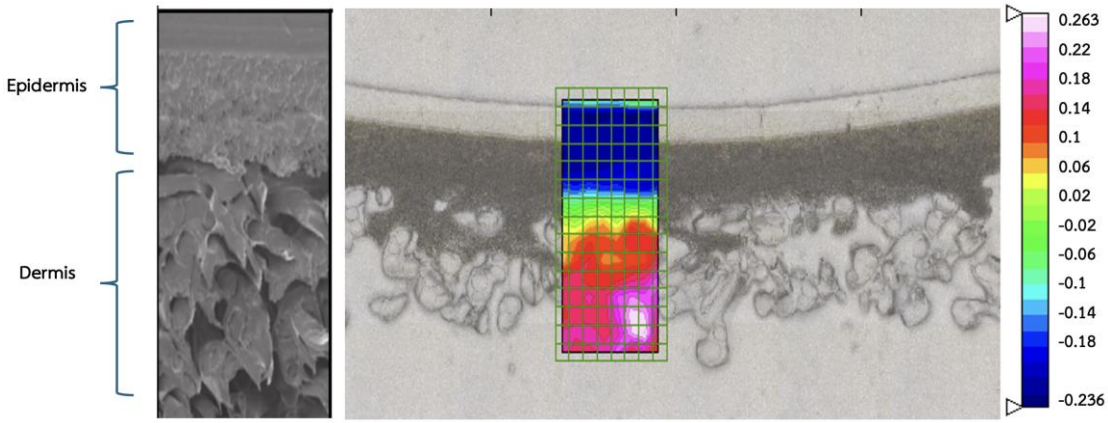

Figure 4.20 FTIR Imaging and Spectral Mapping of Strat-M™ Membrane at Various Time Points (4 hr) in Franz Diffusion Cell System

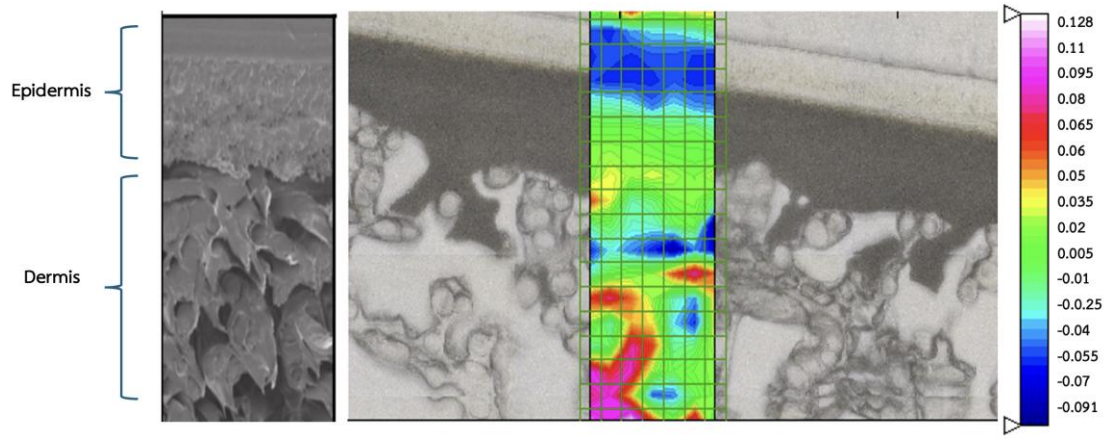

Figure 4.21 FTIR Imaging and Spectral Mapping of Strat-M™ Membrane at Various Time Points (6 hr) in Franz Diffusion Cell System

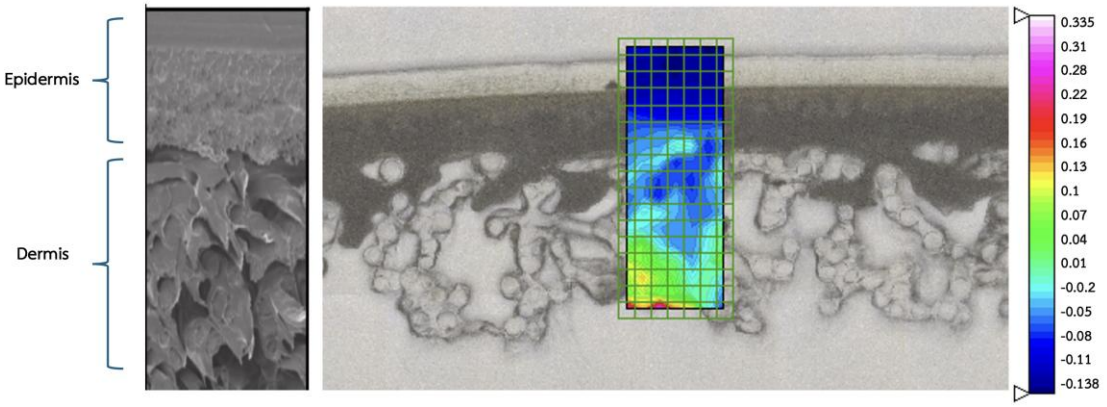

Figure 4.22 FTIR Imaging and Spectral Mapping of Strat-M™ Membrane at Various Time Points (8 hr) in Franz Diffusion Cell System

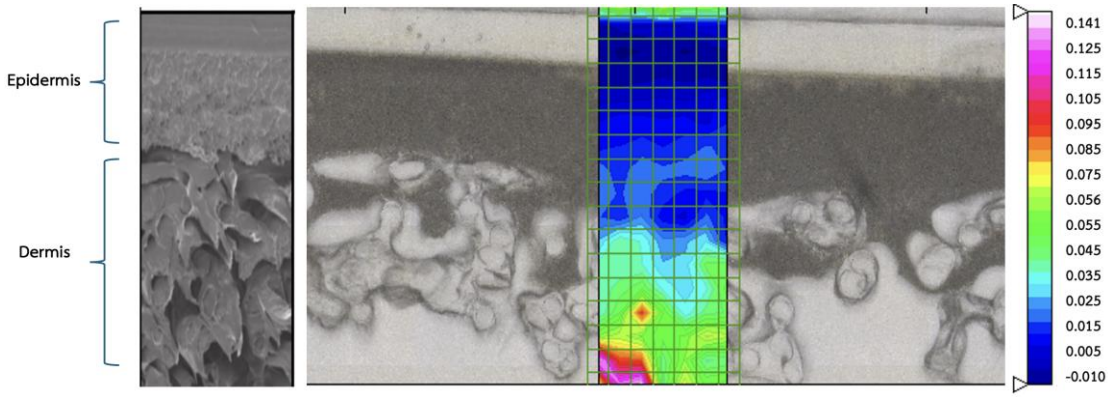

Figure 4.23 FTIR Imaging and Spectral Mapping of Strat-M™ Membrane at Various Time Points (12 hr) in Franz Diffusion Cell System

Figures 4.17-4.23 Representative FTIR images and corresponding spectral mapping at time intervals following application of the capsaicin formulation. Each panel includes the chemical intensity heatmap, selected spatial, and FTIR spectra of the mapped areas showing variations in intensity over time. The progressive diffusion of capsaicin is observed as signal penetration increases into deeper layers.

4.2 Discussion

The successful development of a capsaicin-loaded nanofiber patch using electrospinning technology presents a significant advancement in transdermal drug delivery systems. Capsaicin, a hydrophobic compound known for its analgesic and anti-inflammatory properties, poses formulation challenges due to its low water solubility and potential for skin irritation at high doses. In this study, encapsulating capsaicin in a hydrophilic polymer matrix composed of PVA and PVP proved to be an effective strategy to overcome these limitations. The blend not only improved the solubility and dispersion of capsaicin but also allowed for the formation of smooth, uniform nanofibers with desirable mechanical and morphological characteristics.

The FT-IR spectral analysis provided strong evidence for the physical entrapment of capsaicin within the nanofiber matrix. The observed shifts and broadening of O–H and C=O peaks suggest hydrogen bonding interactions between the drug and polymer, which are favorable for sustained release without compromising the drug's bioactivity. These findings are consistent with previous studies that have demonstrated the ability of PVA and PVP to form hydrogen bonds with small molecules, thus enhancing drug stability and retention within the fiber structure (Hindi et al., 2021).

The FT-IR spectrum of pure capsaicin exhibited a broad absorption peak at approximately 3300 cm^{-1}, corresponding to O–H stretching vibrations indicative of phenolic hydroxyl groups. Additional prominent bands at 2923 cm^{-1} and 2854 cm^{-1} were attributed to asymmetric and symmetric C–H stretching vibrations of aliphatic CH_2 and $–CH_3$ groups (Prietto et al., 2018), respectively. A sharp peak observed at approximately 1640 cm^{-1} was assigned to C=O stretching of the amide group, while signals in the region of 1510–1450 cm^{-1} were characteristic of aromatic C=C ring

stretching. Furthermore, peaks near 1260 cm^{-1} and 1020 cm^{-1} were assigned to C–N and C–O stretching, respectively, confirming the distinct functional groups of capsaicin, consistent with previous reports (Cortés-Estrada et al., 2020; Rezazadeh et al., 2022).

In comparison, the FT-IR spectrum of the capsaicin-loaded nanofiber patch (Figure 4.2B) demonstrated several overlapping and slightly shifted peaks, suggesting the successful incorporation of capsaicin into the polymeric matrix. The broad O–H stretching band around 3300 cm^{-1} was retained but became noticeably broader, indicating the presence of hydrogen bonding interactions between capsaicin and the polymeric components, particularly PVA and PVP (Hashmi et al., 2020). Aliphatic C–H stretching peaks at 2925 cm^{-1} and 2850 cm^{-1} were also observed, further confirming the presence of capsaicin within the nanofiber structure (Amna et al., 2019).

Importantly, the carbonyl stretching band at 1640 cm^{-1} exhibited a slight shift and broadening in the nanofiber spectrum, implying potential physical interactions between capsaicin and the hydroxyl or carbonyl groups within the polymer matrix. These interactions suggest molecular entrapment of capsaicin rather than covalent bonding, a favorable condition for maintaining the pharmacological activity of the compound and enabling a controlled drug release mechanism (Mondal et al., 2019; Tanadchangsaeng et al., 2016).

Additionally, in the fingerprint region (1200–700 cm^{-1}), characteristic peaks associated with the PVP and PVA backbone such as C–O, C–C, and C–N stretching vibrations remained clearly visible (Tahir et al., 2024). This observation confirmed the structural integrity of the polymer network following the electrospinning process. Notably, no new peaks or significant spectral changes were observed, indicating that capsaicin remained chemically stable and did not undergo degradation during fabrication.

The surface morphology of the capsaicin-loaded nanofibers, as examined by scanning electron microscopy (SEM), revealed critical insights into the structural properties of the electrospun fibers (Figure 4.3A). The SEM micrograph, captured at 5,000× magnification, demonstrated that the fibers were smooth, continuous, and free of beads, indicating a homogenous polymer solution and optimal electrospinning parameters. The random yet uniform distribution of fibers across the membrane

suggests favorable morphological conditions for consistent drug release and mechanical integrity in transdermal applications.

Quantitative analysis of fiber diameters, conducted using ImageJ software (NIH, USA), based on measurements of 50 randomly selected fibers (Mitxelena-Iribarren et al., 2023), is presented in Figure 4.4B. The diameter distribution followed a unimodal, slightly right-skewed pattern, with a mean diameter of 0.667 ± 0.195 μm (667 ± 19.5 nm), placing the fibers well within the nanoscale range of 1–1000 nm. This observation confirms the successful formation of true nanofibers, consistent with previous findings on electrospun drug-loaded systems (Hindi et al., 2021).

The relatively narrow standard deviation indicates a high degree of uniformity in fiber thickness, which is essential for maintaining consistent surface area for drug diffusion, mechanical stability, and flexibility of the transdermal patch. The absence of bead formation further suggests favorable polymer solvent interactions and the use of appropriate electrospinning voltage and flow rate settings (Martínez-Ortega et al., 2019). These features collectively support the robustness of the fabrication process and the physicochemical compatibility of the CAP/PVA/PVP system. When compared to other capsaicin-loaded nanofiber systems reported in the literature, the fiber diameters observed in this study are comparable or smaller, which may result in an enhanced surface-area-to-volume ratio (Martínez-Ortega et al., 2019).

The morphological analysis via SEM revealed that the fabricated nanofibers had a narrow diameter distribution, with an average size of approximately 667 nm. This nanoscale size is optimal for dermal applications, as it facilitates close contact with the skin, enhances drug absorption through increased surface area, and contributes to the flexibility and adherence of the patch. Similar findings have been reported, indicating that nanofibers with diameters in the nanoscale range provide a large specific surface area and highly porous structures, which are beneficial for transdermal drug delivery systems (Ahmadi Bonakdar & Rodrigue, 2024). Importantly, the absence of bead formation and the uniformity of the fibers indicate optimal electrospinning conditions, suggesting that the chosen polymer concentration, solvent system, and electrospinning parameters were well-balanced to yield high-quality nanofibers (Al-Abduljabbar & Farooq, 2023).

This characteristic is particularly beneficial for improving drug dispersion and skin permeation efficiency. Overall, the morphological attributes of the developed nanofibers affirm their suitability as a platform for transdermal drug delivery applications.

The cytotoxicity of the capsaicin-loaded nanofiber patch was assessed on human dermal fibroblast (HDF) cells using the MTT assay, and the results are presented in Figure 4.5. Cells were exposed to varying concentrations of nanofiber extract (ranging from 0.0001 to 100 mg/mL) for 24 hours to determine the concentration-dependent effects on cell viability. At lower concentrations (0.0001–1 mg/mL), the nanofiber extract did not exhibit significant cytotoxic effects. Notably, at concentrations of 0.001 and 0.01 mg/mL, a significant increase in cell viability was observed ($p < 0.001$), with viability exceeding 130% relative to the untreated control group. These results suggest that low concentrations of the nanofiber extract may not only be safe but could also enhance fibroblast activity or exert mild protective effects (Ahmady et al., 2023). This effect is likely attributed to the antioxidant and anti-inflammatory properties of capsaicin at sub-cytotoxic concentrations, which may promote cell health and tissue repair.

In contrast, at higher concentrations (10–100 mg/mL), a dose-dependent reduction in cell viability was observed. Specifically, cell viability decreased to approximately 75% at 50 mg/mL and further declined to approximately 40% at 100 mg/mL ($p < 0.001$), indicating significant cytotoxic effects at elevated doses. The dose–response curve allowed for the estimation of the half-maximal inhibitory concentration (IC_{50}), which was determined to be approximately 20 mg/mL. This value represents the concentration at which capsaicin induces a 50% reduction in cell viability under the in vitro conditions used in this study. Similar cytotoxic effects of capsaicin have been reported in previous studies. For instance, Kim et al. demonstrated that capsaicin was toxic to human skin fibroblasts, reducing survival rates to 25–50% after 24 hours of treatment (Chittasupho et al., 2020; Kim et al., 2004). Additionally, research by Szoka & Palka found that capsaicin exhibited cytotoxicity in fibroblasts, with an IC_{50} value of approximately 314.8 ± 14.1 μM at 48 hours of treatment (Szoka & Palka, 2020). These

findings underscore the importance of carefully optimizing capsaicin concentrations in therapeutic applications to balance efficacy and safety.

The IC_{50} value provides a critical reference for defining the upper safety limits in formulation development. Importantly, the concentrations exhibiting cytotoxicity (≥10 mg/mL) are much higher than those typically encountered in transdermal delivery applications. In vivo, the localized concentrations of capsaicin on the skin surface are significantly lower, due to controlled release mechanisms and limited permeation. For example, clinical formulations of capsaicin patches, such as those containing 0.025–0.1% w/w, correspond to microgram-per-milliliter concentrations once applied to the skin, which are well below the observed IC_{50} threshold.

Therefore, the capsaicin nanofiber patch demonstrates a broad safety margin for dermal applications, with effective concentrations for pain relief expected to remain within the non-cytotoxic range *in vivo*. These findings confirm the biocompatibility of the capsaicin-loaded nanofiber patch and support its potential for further development as a safe and effective transdermal therapeutic system.

The protective and restorative effects of the capsaicin-loaded nanofiber patch on human dermal fibroblast (HDF) morphology under oxidative stress conditions were evaluated using phase-contrast microscopy (Figure 4.6). In the untreated control group, HDF cells maintained a typical spindle-shaped fibroblastic morphology, with clearly defined cell borders, healthy cytoplasmic structure, and strong adherence to the culture surface features indicative of intact cellular integrity and normal physiological function.

Upon exposure to 1 mM hydrogen peroxide (H_2O_2) (de Oliveira-Marques et al., 2007), cells exhibited pronounced morphological alterations, including shrinkage, elongation, cytoplasmic condensation, and partial detachment from the culture surface. These changes are characteristic of oxidative stress-induced damage and are consistent with prior reports on H_2O_2-induced cellular inflammation and apoptotic responses in fibroblast models. Such morphological deterioration reflects the detrimental effects of reactive oxygen species (ROS) on cellular structure and function.

Remarkably, treatment with the capsaicin-loaded nanofiber patch at a concentration of 0.1 mg/mL following H_2O_2 exposure resulted in a visible restoration

of fibroblastic morphology. The treated cells appeared more elongated, retained better adhesion, and exhibited fewer structural abnormalities compared to the H_2O_2-only group. These observations suggest that the capsaicin nanofiber formulation conferred a protective or restorative effect on fibroblasts under oxidative stress. This aligns with studies indicating that capsaicin possesses antioxidant properties, reducing oxidative stress and promoting cell survival in various cell types (Zhang et al., 2024).

The morphological recovery observed in this group is in agreement with the anti-inflammatory profile indicated by *COX-2* gene expression levels, as assessed via qRT-PCR. Together, these findings support the cytoprotective and anti-inflammatory potential of capsaicin when delivered through a nanofiber-based transdermal system. The results further highlight the therapeutic relevance of this formulation in mitigating oxidative stress-related cellular damage in skin tissue models.

The anti-inflammatory efficacy of the nanofiber patch was substantiated by the significant reduction in *COX-2* expression following oxidative stress induction with hydrogen peroxide. This suppression is consistent with capsaicin's known mechanism of action, including the inhibition of *COX-2* synthesis via modulation of NF-**K**B and MAPK signaling pathways. Studies have demonstrated that capsaicin effectively inhibits the production of pro-inflammatory mediators such as *COX-2* by suppressing NF-**K**B activation in lipopolysaccharide-stimulated cells (Zheng et al., 2018). Additionally, capsaicin has been shown to affect macrophage anti-inflammatory activity through the modulation of MAPK and NF-**K**B signaling pathways (Li et al., 2021).

Notably, the sustained delivery offered by the nanofiber system may prolong capsaicin's interaction with target cells, thereby enhancing its anti-inflammatory potential compared to conventional topical creams or gels that often suffer from rapid drug clearance and poor skin penetration (Esentürk Güzel et al., 2022). Research indicates that nano-sized carriers can improve the bioavailability and absorption of capsaicinoids, thereby enhancing their anti-inflammatory and analgesic effects (Nava-Ochoa et al., 2021). Furthermore, nanofiber-based delivery systems have been shown to enhance the skin permeability and therapeutic efficacy of capsaicin, suggesting a promising approach for transdermal applications (Ghiasi et al., 2019).

Microscopic evaluation of cell morphology further demonstrated the patch's protective effects. Cells exposed to oxidative stress showed classical signs of damage, including shrinkage and detachment, whereas those treated with the capsaicin patch maintained structural integrity and normal morphology. These observations suggest not only anti-inflammatory effects, but also potential cellular recovery or protection facilitated by the formulation.

The present study investigated the transdermal permeation profile of capsaicin over a 12-hour period using HPLC analysis. Capsaicin was consistently detected across all time intervals (1–12 hours), with a steady increase in peak intensity over time, indicating continuous drug permeation. The observed retention times (approximately 22.3–22.6 minutes) and sharp chromatographic peaks suggest both the chemical stability of capsaicin and the reliability of the analytical method.

These results align with previous research findings. For instance, P. Anantaworasakul et al. (2020) demonstrated that capsaicin could successfully permeate skin layers and accumulate in both the stratum corneum and deeper tissues following topical application. Similarly, a study by Kleber et al. (2014) using Strat-M™ membranes and Franz diffusion cells showed that capsaicin-loaded nanoemulsions with particle sizes ranging from 20 to 62 nm penetrated the membrane layers effectively, supporting the suitability of such models in transdermal delivery evaluations (Kim et al., 2014).

Compared to prior research, the current study further confirms that electrospun or film-formulated capsaicin delivery systems enable sustained release across a prolonged period. In earlier studies utilizing low-concentration capsaicin creams, drug retention was often limited by formulation instability or rapid clearance. In contrast, the formulation tested in this study maintained a progressive release rate, similar to the findings reported by László et al. (2022), who observed that capsaicin-loaded silicone-based TTS formulations provided continuous drug delivery for 12 hours in animal models(Latif et al., 2022). Additionally, the HPLC results presented here corroborate findings from Qutenza™ patch studies, where the 8% capsaicin formulation achieved localized dermal uptake without significant systemic distribution, ensuring sustained therapeutic effect with minimal adverse reactions. While previous work

primarily focused on end-point measurements (e.g., skin deposition after several hours), this study contributes dynamic, time-resolved insight into the release kinetics and chemical stability of capsaicin over time. Taken together, these findings not only reinforce the potential of transdermal systems for capsaicin delivery but also highlight the compatibility of HPLC in evaluating temporal drug release and permeation behavior. Further quantitative assessment of capsaicin concentration at each time point, as well as in vivo confirmation, would strengthen these results and provide clinical relevance for pain management or anti-inflammatory applications.

The FTIR microspectroscopic analysis provided spatial and temporal insights into the diffusion behavior of capsaicin through the Strat-M™ membrane over a 12-hour period. The results clearly demonstrate progressive penetration of capsaicin, with characteristic spectral changes correlating with increased diffusion depth and chemical interaction over time.

At the early stage (1 hour), FTIR spectral signals were primarily localized in the upper membrane layers, as evidenced by strong absorption bands near 2920–2850 cm^{-1} (C–H stretching) and 1650–1500 cm^{-1} (amide and aromatic ring vibrations). These results suggest initial adsorption of capsaicin onto the surface of the membrane without significant diffusion. This surface localization is consistent with prior findings that highlight the stratum corneum-like barrier function of the upper Strat-M™ membrane. By 2 to 4 hours, spectral intensity began to shift deeper into the membrane, with notable increases in C–O and C–N stretching peaks in the 1250–1000 cm^{-1} region. These findings support earlier studies indicating that capsaicin exhibits moderate lipophilicity, allowing gradual partitioning into mid-layers mimicking the viable epidermis. This trend aligns with the permeation kinetics who observed delayed but steady penetration of capsaicin through synthetic and porcine membranes.

At 6 hours, prominent signals at 1510 cm^{-1} (aromatic C=C) and 1100 cm^{-1} (ether C–O) indicate that capsaicin reached deeper, dermis-like layers of the membrane. The associated heatmaps show widespread distribution and increased intensity, suggesting sustained release from the patch and effective translocation across membrane strata. These findings corroborate the sustained-release behavior observed in nanofiber-based capsaicin patches, as described by László et al. (2022).

Notably, the FTIR spectra at 8 and 12 hours revealed peak broadening and intensity stabilization in the 1000–1100 cm^{-1} region, indicative of molecular accumulation and possible interaction with deeper membrane components. This plateauing effect suggests that capsaicin achieved full-depth permeation, consistent with the final phase of Franz diffusion profiles. Comparatively, untreated control membranes displayed negligible chemical signals, further validating the specificity and extent of capsaicin permeation in treated samples.

Overall, the FTIR imaging technique effectively visualized the dynamic and spatial evolution of capsaicin diffusion. The observed spectral shifts and intensity distributions correspond well with capsaicin's chemical structure and known pharmacokinetics in skin models. These findings highlight the value of FTIR spectral mapping in transdermal drug delivery research and support the potential of capsaicin-loaded patches for achieving deep skin penetration and sustained release, crucial for managing localized and pain. Additionally, electrospun nanofibers allow for site-specific delivery, minimizing systemic exposure and side effects.

The calculated permeability coefficient (K_p) of capsaicin demonstrated a distinct time-dependent decline throughout the 12-hour permeation study. The initial high K_p value observed at the 1-hour time point (~0.77 cm/hr) can be attributed to a steep concentration gradient between the donor and receptor compartments, which is known to facilitate rapid transdermal diffusion. This observation is consistent with Fick's First Law of Diffusion, which states that the diffusion flux is directly proportional to the concentration gradient across the membrane (Bajaj et al., 2011; Wokovich et al., 2006).

As time progressed, K_p values declined, reaching a quasi-steady state after 6 hours. This decrease likely reflects both the depletion of surface drug content and the reduction in the driving force for diffusion, as the system approaches equilibrium. Additionally, saturation of the membrane and polymer relaxation within the nanofiber structure may contribute to the gradual attenuation of drug permeation.

Such a biphasic permeation pattern comprising an initial burst followed by sustained releaseis characteristic of electrospun nanofiber drug delivery systems, which are designed to provide both immediate and long-acting therapeutic effects (Hindi et

al., 2021; Vatankhah, 2018). This is particularly advantageous for transdermal applications targeting chronic pain or inflammation, where rapid onset followed by consistent therapeutic levels is desired.

When compared to conventional topical formulations such as gels or creams, which often suffer from poor permeation and uncontrolled release, the nanofiber patch exhibited superior performance in terms of both early-stage permeability and sustained release kinetics. Similar findings were reported by Rezazadeh et al. (2022) (Rezazadeh et al., 2022), who demonstrated enhanced transdermal delivery of capsaicin using zein-based nanofibers, albeit with lower initial K_p values (0.045–0.075 cm/hr).

In summary, the permeability profile obtained from this study supports the hypothesis that the capsaicin-loaded nanofiber patch functions as an efficient and controlled transdermal drug delivery system, capable of enhancing skin permeation and maintaining therapeutic levels of the drug over extended periods.

Despite these promising outcomes, this study also highlights areas for future research. *In vivo* evaluations are necessary to fully assess pharmacokinetics, drug permeation, and long-term therapeutic efficacy. Additionally, studies investigating the sensory effects (e.g., initial burning sensation) associated with capsaicin patches, skin irritation potential, and user acceptability will be critical for clinical translation. Furthermore, scaling up the production process while maintaining uniformity and quality will be essential for commercialization.

In conclusion, the CAP/PVA/PVP nanofiber patch developed in this study exhibits excellent physicochemical properties, safety, and biological activity, making it a strong candidate for further development as a non-invasive treatment for localized pain and inflammation. Its ability to deliver capsaicin in a sustained and biocompatible manner could address current limitations in topical analgesic therapy and open new avenues for nanofiber-based biomedical applications.